

Diurnal and Seasonal Variations of Ultrafine Particle Formation in Anthropogenic SO₂ Plumes

FANGQUN YU*

Atmospheric Sciences Research Center, State University of New York, Albany, New York 12203

Received October 22, 2009. Revised manuscript received December 23, 2009. Accepted February 2, 2010.

The cloud condensation nuclei concentrations predicted by global aerosol models are sensitive to how new particle formation in subgrid anthropogenic SO₂ plumes is parameterized. Using a state-of-the-art kinetic nucleation model, we carried out two case studies to investigate the large difference in the number concentrations of ultrafine particles observed in the plumes from the Horne smelter: one in the summer and the other in the winter. Our model predicted that particle number concentrations are in good agreement with observations for both cases, showing that particle formation in the Horne smelter plumes is dominated by binary homogeneous nucleation (BHN) in the winter case and by ion-mediated nucleation (IMN) in the summer case. Further sensitivity studies reveal significant diurnal and seasonal variations of sulfate particle formation in the anthropogenic SO₂ plume, mainly associated with corresponding variations of two key parameters: hydroxyl radical concentration ([OH]) and temperature. Nucleation in the plume is negligible at night because of very low [OH]. BHN is significant when [OH] is relatively high or temperature is relatively low, and it is generally limited to the fresh plumes (within ~15 km from source), but it can generate very high concentrations of ultrafine particles (peak values as high as 10⁵–10⁶ cm⁻³) under favorable conditions. IMN generally dominates nucleation in the plume when [OH] is relatively low or temperature is relatively high, and it extends from fresh plume to more aged plume and produces 2–3 × 10⁴ cm⁻³ of nucleated particles. The implications of the results are discussed.

Introduction

Aerosol indirect radiative forcing, the most important source of uncertainties in assessing climate change (1), is largely determined by the number abundance of particles that can act as cloud condensation nuclei (CCN). At a given water supersaturation ratio, CCN number concentrations depend on the number size distribution and composition of atmospheric particles. Aerosol particles appear in the troposphere due to either in situ nucleation (i.e., secondary particles) or direct emissions (i.e., primary particles). Most of the recent global aerosol simulations assume that 0–5% of anthropogenic sulfur specie is emitted as sulfuric acid or sulfate and the rest is emitted as SO₂ (2–7). While this fraction of sulfate mass (f_{SO_4}) is called “primary sulfate”, it is actually secondary in nature because it is used to account for subgrid SO₂ oxidation and new particle formation. The above-mentioned

global aerosol simulations show that the simulated tropospheric CCN abundance is sensitive to the parameterization of the new particle formation in subgrid SO₂ plumes (especially in the source regions), and thus it is important to reduce the uncertainties in this parameterization.

Sulfur emission from power plants and smelters is a dominant anthropogenic sulfur source. Thorough airborne sampling of the SO₂ to sulfate conversion rate (r_{sc}) and sulfate particle formation in plumes from coal-fired power plants and smelters was undertaken in the late 1970s and early 1980s. Measurements reported by Wilson and McMurry (8) indicate that the formation of sulfate particles in the power plant plume depends strongly upon the time of day with none observed in plume parcels that were not exposed to sunlight. Wilson (9) reviewed measurements collected in 12 power plant and smelter plumes in Australia, Canada, and the United States, during warm and cold seasons and during days and nights. In spite of the wide geographical, seasonal, background, and source variations, Wilson (9) showed a distinct difference in the observed day and night r_{sc} . The variability is significantly less for plumes with similar exposure to sunlight dose (9), which is consistent with the fact that the dominant route of oxidation of SO₂ in the gas phase is the reaction with the hydroxyl radical (OH) (10, 11). Depending on the OH concentration ([OH]), r_{sc} can vary from ≈1%/h to ≈10%/h (11). It is clear that the fractions of sulfur converted to sulfate during the subgrid plume dilution ($f_{SO_4} = r_{sc} \times \Delta t$) depend on [OH] and have clear diurnal variations. Sulfate particle formation in power plant and smelter plumes has been characterized in a number of more recent field measurements (12–15). Banic et al. (15) showed that the number concentration of ultrafine particles formed in the same smelter plume differs significantly in winter and summer.

In addition to f_{SO_4} , the concentrations and sizes of nucleated particles in subgrid anthropogenic sulfur plumes are also expected to vary significantly. The mass of primary sulfate, calculated from f_{SO_4} and the sulfur emission rate at a given grid box, is generally distributed into two log-normal modes with the geometric mean diameters (d_g) and standard deviations (σ_g) of 10 nm and 1.6 for nucleation mode and 70 nm and 2.0 for condensation mode (16). As it has been pointed out in Yu and Luo (7), most of the global aerosol studies assume that 15% of primary sulfate mass is emitted into the nucleation mode (i.e., $f_{nucl} = 15\%$), while the rest is partitioned into the condensation or accumulation mode. However, the reference cited in these studies (16, 17) showed that f_{nucl} is 5% (instead of widely used 15%), while the remaining sulfate (formed in subgrid SO₂ plumes) condenses directly onto existing particles. Whitby et al. (16) derived the typical values of d_g and σ_g , as well as f_{nucl} , from limited measurements obtained in the Labadie power plant plume near St. Louis, Missouri, in 1976. It is clear that one can expect large uncertainties in these parameters. Actually, Whitby et al. (16) showed that f_{nucl} , derived from measurements obtained in eight different plume crossings, range from 1% to 9%. It should be noted that the primary sulfate mass from the power plant is distributed into a log-normal mode with $d_g = 500$ nm and $\sigma_g = 2.0$ in AeroCom inventory (18), but the physics or reason behind such an assumption is unclear.

As far as we know, all the existing global aerosol studies assume a fixed f_{SO_4} , f_{nucl} , d_g , and σ_g for the whole simulation period over the whole globe (i.e., no diurnal, seasonal, and spatial variations). Such an overly simplified representation of subgrid new particle formation is likely to significantly overpredict the new particle formation in the local night

* Corresponding author phone: (518) 437-8767; e-mail: yfq@asrc.cestm.albany.edu.

time and lead to large uncertainties in the spatiotemporal variations of predicted ultrafine particle number concentration and CCN abundance. The main objective of this study is to improve our understanding of the diurnal and seasonal variations of ultrafine sulfate particle formation in power plant and smelter plumes through case and sensitivity studies. Such an understanding is critical to improve the representation of the subgrid plume scale nucleation process and thus reduce uncertainties in the regional and global simulations of aerosol number abundance that is important for the assessment of aerosol climatic and health impacts.

Methodology

We employ the most recent version of the kinetic ion-mediated nucleation (IMN) model (19), which is suitable for simulating the particle formation and evolution in diluting plumes where key parameters are changing. The IMN model contains binary homogeneous nucleation (BHN), and it reduces to BHN when ion concentration is set to zero or when the nucleation rate is much larger than the ionization rate. The IMN model explicitly solves particle condensation growth and coagulation (including the scavenging of freshly nucleated nanometer-sized particles by pre-existing particles) (19). In the past, the kinetic IMN model has been successfully applied to study particle formation and evolution in the plumes of aircraft exhaust and vehicular exhaust (20, 21). There are five key parameters controlling the new particle formation rate via IMN (22): sulfuric acid vapor concentration ($[H_2SO_4]$), temperature (T), relative humidity (RH), ionization rate (Q), and surface area of background particles (SB). $[H_2SO_4]$ in the power plant plumes depend on SO_2 concentration ($[SO_2]$), $[OH]$, SB, and plume dilution.

To simplify the problem, we treat the plume exhaust as a perturbed parcel of air subject to dilution through mixing with ambient environment. The IMN model is a kinetic particle formation and evolution model, and we run it as a box model along the trajectory of an expanding plume in an approach similar to previous simulations of particle evolution in aircraft plumes (20). The dilution of the exhaust is represented as an increase in the cross-sectional area of the plume by various mixing processes, and all of the constituents in the plume are assumed to be uniformly mixed instantaneously across the entire cross section. While this approximation is obviously crude, it may be rationalized as representing the bulk mean properties of the plume (20). The plume dilution rate depends on the wind speed and boundary layer stability. There exist a number of approaches to calculate the plume dispersion process (23). One key consideration is to specify the horizontal and vertical standard deviations (m) of the Gaussian distribution σ_y and σ_z . In this study, we calculate σ_y and σ_z on the basis of MESOPUFF II stability-dependent dispersion curves (23)

$$\sigma_y = a_y x^{b_y}$$

$$\sigma_z = a_z x^{b_z}$$

where a_y , b_y , a_z , and b_z are the coefficients that depend on the Pasquill-Gifford-Turner (PGT) stability class (Table 2–8 in ref 23). x is the downwind distance.

The initial $[SO_2]$ can be calculated on the basis of the SO_2 emission rate ($kg\ SO_2/h$), initial plume cross-sectional area, and wind speed. Apparently $[SO_2]$ in different plumes is expected to vary significantly due to the difference in the SO_2 source rate and initial plume cross section and dispersion rate. The conversion of SO_2 into sulfuric acid is calculated on the basis of the reactions of SO_2 with OH . It should be noted that $[OH]$ in the concentrated plume stages (plume age ~ 10 s) is generally 2–3 orders of magnitudes lower than

that in the background air because of the depletion of ozone near the source region (24–26). $[OH]$ in the plume approaches $[OH]_{amb}$ around plume age of 300–600 s. Taking this into account, we use the plume age-dependent $[OH]$ profile given in Cocks and Fletcher (24) to scale the $[OH]$ in the fresh plume. Because SO_2 together with $[OH]$ determine the H_2SO_4 production rate, the impact of $[SO_2]$ variations on nucleation at fixed OH can be seen from the impact of $[OH]$ variations at fixed $[SO_2]$.

Results and Discussion

It is apparent from the previous section that many parameters controlling new particle formation in power plant or smelter plumes can have large spatial and temporal variations. The focus of the present study is on the impact of two key parameters controlling the diurnal and seasonal variations of sulfate particle formation in the power plant plume: $[OH]$ and T .

Simulations and Comparisons with Measurements: Case Studies. We first carry out case studies of two flight measurements taken in the plumes from the Horne smelter (one in summer, 7/28/2000, and the other in winter, 2/19/2000 ref 15), aiming to understand the observed large difference in the number concentrations of ultrafine particles formed in the two different seasons. The sulfur emission rate for the Horne smelter is taken from Savard et al. (27). The metrological parameters (T , RH, and wind speed, V), ambient $[OH]$, and surface area of background particles (SB) needed for the plume simulations are based on GEOS-Chem simulations (7). GEOS-Chem uses assimilated meteorological data from the NASA Goddard Earth Observing System and contains many state-of-the-art modules treating various chemical and particle processes (28–30). The values of T , RH, V , $[OH]$, and SB in the Horne smelter region during the periods when measurements were taken (15) are 293 K, 65%, 5 m/s, $2 \times 10^6\ cm^{-3}$, and $140\ \mu\text{m}^2\text{cm}^{-3}$, respectively, on 7/28/2000 (summer case) and 267 K, 78%, 7.5 m/s, $10^6\ cm^{-3}$, and $150\ \mu\text{m}^2\text{cm}^{-3}$, respectively on 2/19/2000 (winter case). The values of T , RH, and V for the two periods are overall consistent with the meteorology data in the region archived at weather underground (<http://www.wunderground.com>). On the basis of assumed size distributions of pre-existing particles (Section 2), SB values of 140 – $150\ \mu\text{m}^2\text{cm}^{-3}$ give a total particle number concentration of $\sim 2400\ cm^{-3}$, consistent with the concentrations of background particles observed in the upper wind (15). The ionization rate is assumed to be $10\ ion\cdot pairs\ cm^{-3}\text{s}^{-1}$ (31). The background aerosol is assumed to have a bimodal log-normal distribution with mean dry diameter and a standard deviation of $d_1 = 60\ nm$, $\sigma_1 = 1.6$ and $d_2 = 200\ nm$, $\sigma_2 = 1.8$. The ratio of total number concentration of mode 1 (N_1) to that of mode 2 (N_2) is assumed to be 100:3, and the exact values of N_1 and N_2 are determined on the basis of assumed SB values. Initial primary particles from combustion (at plume age = 0) are assumed to have a bimodal log-normal distribution with $N_1 = 10^6\ cm^{-3}$, $d_1 = 100\ nm$, $\sigma_1 = 1.6$ and $N_2 = 10^4\ cm^{-3}$, $d_2 = 1000\ nm$, $\sigma_2 = 1.8$ (32), which gives a total surface area of $\sim 10^5\ \mu\text{m}^2\text{cm}^{-3}$. The influence of uncertainties in the assumed ionization rates, size distributions of background particles, and initial plume particles on simulated results is assessed in the Supporting Information.

Figures 1 and 2 show $[SO_2]$, $[H_2SO_4]$, number concentrations of condensation nuclei with diameter larger than 3 nm (CN3) and 15 nm (CN15), and particle number size distributions as a function of plume distances from source (x), simulated with the kinetic IMN model for the two study cases. For comparisons, the observed SO_2 concentrations for the winter case and the observed CN15 for both the winter and summer cases (estimated from Figures 3 and 4 in ref 15) are also marked in panels a and b of Figure 1. No measured

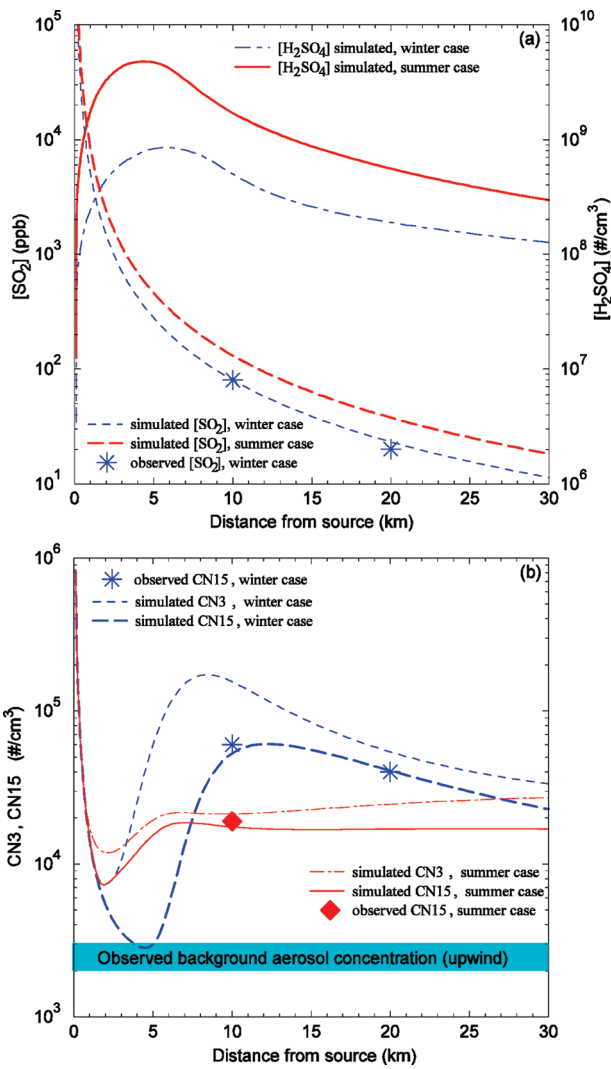


FIGURE 1. Simulated evolution (lines) of [SO₂], [H₂SO₄], and number concentrations of condensation nuclei with diameter larger than 3 nm (CN3) and 15 nm (CN15) in the SO₂ plume from the Horne smelter in two different seasons: one in summer (7/28/2000) and the other in winter (2/19/2000). The symbols are the observed SO₂ concentrations for the winter case and the observed CN15 for both winter and summer cases (estimated from Figures 3 and 4 in ref 15).

values of [SO₂] for the summer case were reported in Banic et al. (15). It is clear that the simulated [SO₂] for the winter case is consistent with measurements at $x = 10$ km and 20 km, suggesting that plume dilution parameterization is reasonable. [SO₂] in the summer case is a factor of ~ 1.5 higher than that in the winter case because of lower wind speed. The particle number concentration in the plume near the source is higher due to emission of primary particles but drops to ambient level within a distance of ~ 3 km from source because of dilution. As a result of higher [SO₂] and [OH] and thus H₂SO₄ production rate, [H₂SO₄] is a factor of ~ 3 higher in the summer case. However, nucleation is much stronger in the winter case due to the lower temperature. In the winter case, the peak value of CN3 reaches 1.7×10^5 cm⁻³ at $x = \sim 8$ km and then decreases gradually as a result of dilution and coagulation. In the summer case, CN3 reaches $\sim 2 \times 10^4$ cm⁻³ at $x = \sim 5$ km and thereafter slightly increases with plume age despite dilution, indicating continuous particle nucleation and growth in the plume (Figure 2b). It is clear from Figure 1 that the predicted CN15 agrees quite well with observations for both seasons, and our model captures the large difference in the observed CN15 between the two

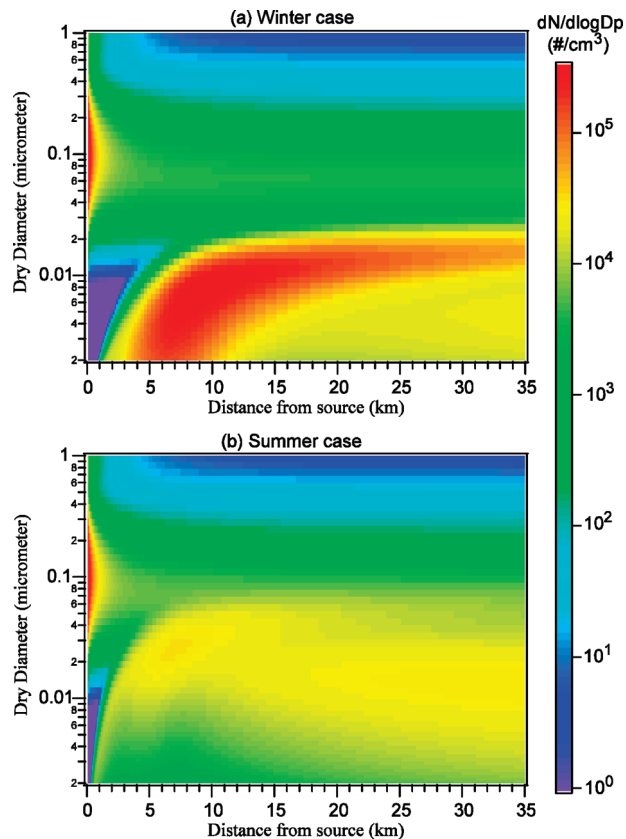


FIGURE 2. Simulated evolution of particle number size distributions for the two cases shown in Figure 1.

seasons. Our model simulations confirm the significant new particle formation in the smelter plume, and total particle number concentrations in the plume can exceed that of background by a factor of ~ 10 or more.

The relative contribution of BHN and IMN to the particles formed in the SO₂ plumes can be determined by setting the ionization rate to zero (Figure S1 in Supporting Information). For the two case studies shown in Figures 1 and 2, our analysis indicates that the particle formation is dominated by BHN in the winter case, while it is dominated by IMN in the summer case. In the winter case, the peak nucleation rate can reach up to ~ 700 cm⁻³s⁻¹ at $x = \sim 6$ km because of lower T, and these nucleated particles grow to ~ 10 nm at $x = 10$ km (Figure 2a). In the summer case, the particle growth rate is larger because of higher [H₂SO₄], and the new particles formed near source ($x < \sim 10$ km) can grow to ~ 40 nm (Figure 2b). At $x > 10$ km, nucleation continues (mainly via IMN) in both cases. Most of the new particles formed at $x > 10$ km in the winter case are scavenged by the large concentration of particles nucleated at $x < 10$ km. In contrast, in the summer case, most of the particles formed at $x > 10$ km grow to a size of ~ 10 nm, and these particles dominate the total particle number concentration at $x = 30$ km (Figure 2b). Figure 2 shows that the nucleation mode particles at $x = 30$ km in both cases have median sizes of ~ 15 nm, slightly larger than the widely used parameterization ($d_g = 10$ nm) given by Whitby et al. (16). It is also clear from Figure 2 that the nucleation mode particle size distributions change as the plume evolves, and the total number concentration and standard deviation of nucleation mode particles differ significantly for the winter and summer cases.

It should be noted that the case study simulations shown in Figures 1 and 2 are subject to some uncertainties associated with the assumed values of some input parameters such as ionization rates, size distributions of background particles, and initial plume particles (Supporting Information). Nev-

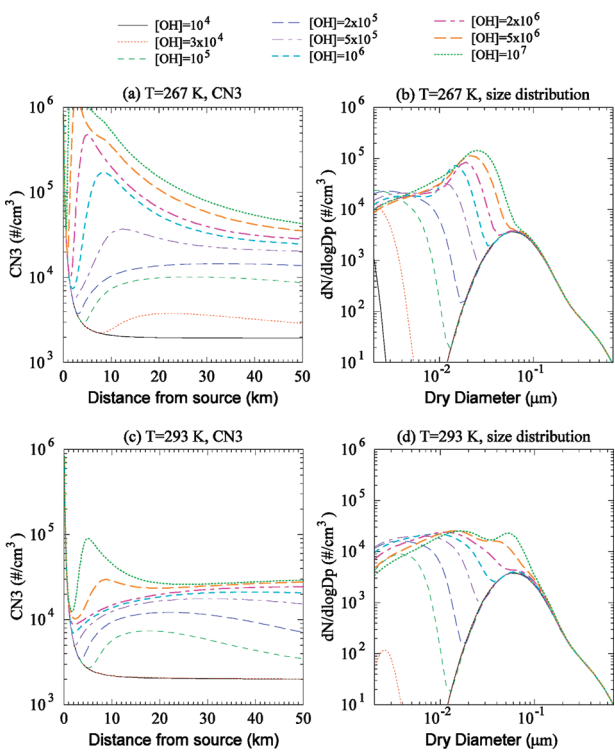


FIGURE 3. Predicted CN3 as a function of distance from source (a, c), and particle size distributions at $x = 30\text{ km}$ (b, d) under nine $[\text{OH}]$ value ranges and two temperatures (267 and 293 K). All other parameters (wind speed, relative humidity, etc.) are assumed to be the same.

ertheless, these uncertainties do not affect our conclusion about the dominance of IMN in the summer case and BHN in the winter case. While SO_2 oxidation rate and hence H_2SO_4 concentration are lower in the winter case, BHN leads to very high nucleation rate as a result of low temperature, which explains why the particle number concentrations observed in the plumes from the Horne smelter in the winter season are much larger than those in the summer case.

Diurnal and Seasonal Variations: Sensitivity Studies. In the two case study simulations shown in Figures 1 and 2, the $[\text{OH}]$ values are close to the peak values during the day. As we pointed out in the Introduction, observations indicate that sulfate particle formation in anthropogenic SO_2 plumes clearly have diurnal variations. $[\text{OH}]$, the key factor controlling the observed diurnal variations, also has large spatial variations, and peak $[\text{OH}]$ concentration can exceed $1 \times 10^7\text{ cm}^{-3}$ at low latitudes. We have carried out sensitivity studies to investigate the impact of the $[\text{OH}]$ values on formation and properties of sulfate particles in an anthropogenic SO_2 plume. Figure 3 shows the predicted CN3 as a function of distance from source (Figure 3a,c) and particle size distributions at $x = 30\text{ km}$ (Figure 3b,d) under nine $[\text{OH}]$ values range from 10^4 – 10^7 cm^{-3} and two temperatures (267 and 293 K). To isolate the effect of T , all other parameters (RH, wind speed, SB, etc.) are assumed to be the same for the simulations shown in panels a and b of Figure 3 and panels c and d of Figure 3.

As expected, $[\text{OH}]$ has a strong impact on new particle formation in a SO_2 plume, not only on the total number concentrations but also on the sizes of nucleated particles. The impact of T can also clearly seen by comparing panels a and b of Figure 3 with panels c and d of Figures 3. Under the assumed conditions, nucleation in the plume is negligible when $[\text{OH}] < \sim 10^4\text{ cm}^{-3}$ at $T = 267\text{ K}$ and when $[\text{OH}] < \sim 3 \times 10^4\text{ cm}^{-3}$ at $T = 293\text{ K}$. A substantial amount of new particles are formed when $[\text{OH}] > \sim 10^5\text{ cm}^{-3}$. IMN generally dominates and produces up to ~ 2 – $3 \times 10^4\text{ cm}^{-3}$ of particles when $[\text{OH}]$

$> \sim 5 \times 10^5\text{ cm}^{-3}$ at $T = 267\text{ K}$ and when $[\text{OH}] < \sim 5 \times 10^6\text{ cm}^{-3}$ at $T = 293\text{ K}$. BHN becomes significant at high $[\text{OH}]$, and levels of $[\text{OH}]$ for BHN to be important depend on T . At $T = 267\text{ K}$ (representing winter condition), BHN can generate large amounts of ultrafine particles when $[\text{OH}] > \sim 5 \times 10^5\text{ cm}^{-3}$, with peak concentrations reaching 10^5 – 10^6 cm^{-3} in the plume within a distance of $\sim 15\text{ km}$ from source. At $T = 293\text{ K}$ (representing summer condition), BHN becomes important when $[\text{OH}] > \sim 5 \times 10^6\text{ cm}^{-3}$, but the degree of nucleation strength is much less than at lower T . BHN is generally limited to the relatively fresh plumes (within $\sim 15\text{ km}$ from source), while IMN continues in the aged plumes, resulting in a bimodal size distribution of nucleated particles (Figures 3b,d). The nucleated particles of larger modes in Figures 3b ($d_g > \sim 10\text{ nm}$) and 3d ($d_g > \sim 30\text{ nm}$) are mainly from BHN (nucleated earlier and have more time to grow), while those of smaller mode result from IMN.

Our case and sensitivity studies show clear diurnal and seasonal variations of new particle formation in anthropogenic SO_2 plumes, mainly as a result of variations in $[\text{OH}]$ and T . While other parameters (such as RH, SO_2 emission rate, wind speed, mixing process, and surface area of pre-existing particles) will also affect particle formation in the SO_2 plumes, their contributions to the diurnal and seasonal variations are expected to be relatively small. In a given SO_2 plume, night time nucleation in the SO_2 plume is negligible because of very low $[\text{OH}]$, and day time nucleation strength depends on $[\text{OH}]$ and T . IMN generally dominates nucleation in the plume when $[\text{OH}]$ is relatively low and T is relatively high, and it can last for several hours and generate 2 – $3 \times 10^4\text{ cm}^{-3}$ of nucleated particles. BHN can become significant when $[\text{OH}]$ is relatively high and T is relatively low, and it is generally limited to the relatively fresh plumes (within $\sim 15\text{ km}$ from source), but it can generate very high concentrations of ultrafine particles (peak values as high as 10^5 – 10^6 cm^{-3}) under certain conditions. The relative and absolute contributions of BHN and IMN to new particles formed in the SO_2 plume mainly depend on T and $[\text{H}_2\text{SO}_4]$, with the latter controlled by $[\text{OH}]$, $[\text{SO}_2]$, and surface area of pre-existing particles in the plume. It should be noted that BHN may become dominant in the summer and IMN in the winter under certain conditions.

Implications. The key processes and parameters controlling the formation and properties of nucleated particles in the anthropogenic SO_2 plumes are poorly understood. The diurnal and seasonal variations of ultrafine sulfate particle formation in power plant and smelter plumes are investigated in the present study, with a state-of-the-art kinetic nucleation model. Our results show that BHN, while is generally unimportant to particle formation in the ambient atmosphere, can lead to very large concentrations ($> 10^5\text{ cm}^{-3}$) of ultrafine particles in relatively fresh anthropogenic SO_2 plumes under suitable conditions (low T , high $[\text{OH}]$). It should be noted that the BHN component of the IMN model, on which the current research is based, is constrained by multiple independent laboratory data sets and has much smaller uncertainty compared to previous BHN models (33). Ammonia and certain organic species are known to enhance BHN, and it remains to be investigated how much these species can enhance nucleation in anthropogenic SO_2 plumes. More comparisons of theoretical predictions with detailed measurements are needed to further advance our understanding of the nucleation process in anthropogenic SO_2 plumes.

Our case and sensitivity studies indicate that the concentrations and sizes of ultrafine sulfate particles formed in anthropogenic SO_2 plumes have large temporal (diurnal and seasonal) and spatial variations. Previous global aerosol studies assuming fixed (i.e., no spatiotemporal variations) parameterizations of subgrid new particle formation in the

anthropogenic SO₂ plume are subject to large uncertainties in the predicted ultrafine particle number concentration and CCN abundance near source regions. Further research is needed to develop suitable parameterization of subgrid plume scale new particle formation, which considers its spatiotemporal variations. Application of such parameterization is necessary to improve the ability of regional and global size-resolved aerosol models in predicting spatiotemporal variations of aerosol number concentration and CCN abundance, which is important for assessing aerosol climatic and health impacts.

Acknowledgments

This study is supported by NSF under grant AGS-0942106 and NASA under grant NNX08AK48G.

Supporting Information Available

Table S1 contains the values assumed in the baseline and sensitivity study cases for the following parameters: surface area of background aerosol, the ratio of the total number concentration of mode 1 to that of mode 2 of background aerosol, surface area of initial particles in the plume, and ionization rate. Figure S1 shows the influence of uncertainties in the above-mentioned parameters on the simulated evolution of particle number concentrations in the SO₂ plume from the Horne smelter: one in summer and the other in winter. This material is available free of charge via the Internet at <http://pubs.acs.org>.

Literature Cited

- (1) IPCC. *Climate Change 2007: The Physical Scientific Basis*; Solomon, S., Qin, D. et al., Eds.; Cambridge University Press: New York, 2007.
- (2) Adams, P. J.; Seinfeld, J. H. Disproportionate impact of particulate emissions on global cloud condensation nuclei concentrations. *Geophys. Res. Lett.* **2003**, *30*, 1239, doi:10.1029/2002GL016303.
- (3) Spracklen, D. V.; Pringle, K. J.; Carslaw, K. S.; Chipperfield, M. P.; Mann, G. W. A global off-line model of size-resolved aerosol microphysics: II. Identification of key uncertainties. *Atmos. Chem. Phys.* **2005**, *5*, 3233–3250.
- (4) Pierce, J. R.; Adams, P. J. Global evaluation of ccn formation by direct emission of sea salt and growth of ultrafine sea salt. *J. Geophys. Res.* **2006**, *111*, D06203, doi:10.1029/2005JD006186.
- (5) Makkonen, R.; Asmi, A.; Korhonen, H.; Kokkola, H.; Järvenoja, S.; Räisänen, P.; Lehtinen, K. E. J.; Laaksonen, A.; Kerminen, V.-M.; Järvinen, H.; et al. Sensitivity of aerosol concentrations and cloud properties to nucleation and secondary organic distribution in ECHAM5-HAM global circulation model. *Atmos. Chem. Phys.* **2009**, *9*, 1747–1766.
- (6) Wang, M.; Penner, J. E. Aerosol indirect forcing in a global model with particle nucleation. *Atmos. Chem. Phys.* **2009**, *9*, 239–260.
- (7) Yu, F.; Luo, G. Simulation of particle size distribution with a global aerosol model: Contribution of nucleation to aerosol and CCN number concentrations. *Atmos. Chem. Phys.* **2009**, *9*, 7691–7710.
- (8) Wilson, J. C.; McMurry, P. H. Studies of aerosol formation in power plant plumes. II. Secondary aerosol formation in the Navajo Generating Station plume. *Atmos. Environ.* **1981**, *15*, 2329–2339.
- (9) Wilson, W. E. Sulfate formation in point source plumes: A review of recent studies. *Atmos. Environ.* **1981**, *15*, 2573–2581.
- (10) Hegg, D. A.; Hobbs, P. V. Measurements of gas-to-particle conversion in the plumes from five coal-fired electric power plants. *Atmos. Environ.* **1980**, *14*, 99–116.
- (11) Hewitt, C. N. The atmospheric chemistry of sulphur and nitrogen in power station plumes. *Atmos. Environ.* **2001**, *35*, 1155–1170.
- (12) Brock, C. A.; Trainer, M.; Byerson, T. B.; Neuman, J. A.; Parrish, D. D.; Holloway, J. S.; Nicks, D. K., Jr.; Frost, G. J.; Hübler, G.; Fehsenfeld, F. C.; et al. Particle growth in urban and industrial plumes in Texas. *J. Geophys. Res.* **2003**, *108*, 4111, doi:10.1029/2002JD002746.
- (13) Brock, C. A.; Washenfelder, R. A.; Trainer, M.; Byerson, T. B.; Wilson, J. C.; Reeves, J. M.; Huey, L. G.; Holloway, J. S.; Parrish, D. D.; Hübler, G.; Fehsenfeld, F. C. Particle growth in the plumes of coal-fired power plants. *J. Geophys. Res.* **2002**, *107* (D12), 4155, doi:10.1029/2001JD001062.
- (14) Springston, S. R.; Kleinman, L. I.; Brechtel, F.; Lee, Y. N.; Nunnermacker, L. J.; Wang, J. Chemical evolution of an isolated power plant plume during the TexAQS 2000 study. *Atmos. Environ.* **2005**, *39*, 3431–3443.
- (15) Banic, C.; Leaitch, W. R.; Strawbridge, K.; Tanabe, R.; Wong, H.; Gariépy, C.; Simonetti, A.; Nejedly, Z.; Campbell, J. L.; Lu, J.; et al. The physical and chemical evolution of aerosols in smelter and power plant plumes: An airborne study. *Geochem.: Explor., Environ.* **2006**, *6*, 111–120.
- (16) Whitby, K. T.; Cantrell, B. K.; Kittelson, D. B. Nuclei formation rates in a coal-fired power plant plume. *Atmos. Environ.* **1978**, *12*, 313–321.
- (17) Whitby, K. The physical characteristics of sulfur aerosols. *Atmos. Environ.* **1978**, *12*, 135–159.
- (18) Dentener, F.; Kinne, S.; Bond, T.; Boucher, O.; Cofala, J.; Generoso, S.; Ginoux, P.; Gong, S.; Hoelzemann, J. J.; Ito, A.; et al. Emissions of primary aerosol and precursor gases in the years 2000 and 1750 prescribed data sets for AeroCom. *Atmos. Chem. Phys.* **2006**, *6*, 4321–4344.
- (19) Yu, F. From molecular clusters to nanoparticles: Second-generation ion-mediated nucleation model. *Atmos. Chem. Phys.* **2006**, *6*, 5193–5211.
- (20) Yu, F.; Turco, R. P. The formation and evolution of aerosols in stratospheric aircraft plumes: Numerical simulations and comparisons with observations. *J. Geophys. Res.*, **1998**, *103*, 25,915–25,934.
- (21) Yu, F. Chemiions and nanoparticle formation in diesel engine exhaust. *Geophys. Res. Lett.* **2001**, *28*, 4191–4194.
- (22) Yu, F. Ion-mediated nucleation in the atmosphere: Key controlling parameters, implications, and look-up table. *J. Geophys. Res.* **2010**, *115*, D03206, doi:10.1029/2009JD012630.
- (23) Scire, J.; Strimaitis, D. G.; Yamartino, R. J. A User's Guide for the CALPUFF Dispersion Model, Version 5; 2000.
- (24) Cocks, A. T.; Fletcher, I. S. Major factors influencing gas-phase chemistry in power plant plumes during long range transport. II. Release time and dispersion rate for dispersion into an “urban” ambient atmosphere. *Atmos. Environ.* **1989**, *23*, 2801–2812.
- (25) Janssen, L. H. J. M.; Nieuwstadt, F. T. M.; Donze, M. Time scales of physical and chemical processes in chemically reactive plumes. *Atmos. Environ.* **1990**, *24A*, 2861–2874.
- (26) Kerminen, V. M.; Wexler, A. S. The occurrence of sulfuric acid–water nucleation in plumes: Urban environment. *Tellus* **1996**, *48B*, 65–82.
- (27) Savard, M. M.; Bonham-Carter, G. F.; Banic, C. M. A geoscientific perspective on airborne smelter emissions of metals in the environment: An overview. *Geochem.: Explor., Environ., Anal.* **2006**, *6*, 99–109.
- (28) Bey, I.; Jacob, D. J.; Yantosca, R. M.; Logan, J. A.; Field, B.; Fiore, A. M.; Li, Q.; Liu, H.; Mickley, L. J.; Schultz, M. Global modeling of tropospheric chemistry with assimilated meteorology: Model description and evaluation. *J. Geophys. Res.* **2001**, *106*, 23073–23096.
- (29) Park, R. J.; Jacob, D. J.; Field, B. D.; Yantosca, R. M.; Chin, M. Natural and transboundary pollution influences on sulfate–nitrate–ammonium aerosols in the United States: Implications for policy. *J. Geophys. Res.* **2004**, *109*, D15204, doi:10.1029/2003JD004473.
- (30) Evans, M. J.; Jacob, D. J. Impact of new laboratory studies of N₂O₅ hydrolysis on global model budgets of tropospheric nitrogen oxides, ozone, and OH. *Geophys. Res. Lett.* **2005**, *32*, L09813.
- (31) Reiter, R. *Phenomena in Atmospheric and Environmental Electricity*; Elsevier: New York, 1992.
- (32) Moisio, M.; Laitinen, A.; Hautanen, J.; Keskinen, J. Fine particle size distributions of seven different combustion power plants. *J. Aerosol Sci.* **1998**, *29* (Suppl. 1), S459–S460.
- (33) Yu, F. An improved quasi-unary nucleation model for binary H₂SO₄–H₂O homogeneous nucleation. *J. Chem. Phys.* **2007**, *127*, 054301.

ES903228A